DEVELOPMENT AND DISEASE

A genetic link between *Tbx1* and fibroblast growth factor signaling

Francesca Vitelli[1], Ilaria Taddei[1], Masae Morishima[1], Erik N. Meyers[2], Elizabeth A. Lindsay[1] and Antonio Baldini[1,3]

[1]Department of Pediatrics (Cardiology), Baylor College of Medicine, Houston TX 77030, USA
[2]Department of Pediatrics and Cell Biology, Duke University Medical Center, Durham NC 27710, USA
[3]Department of Molecular and Human Genetics, Baylor College of Medicine, Houston TX 77030, USA
*Author for correspondence (e-mail: baldini@bcm.tmc.edu)

SUMMARY

Tbx1 haploinsufficiency causes aortic arch abnormalities in mice because of early growth and remodeling defects of the fourth pharyngeal arch arteries. The function of *Tbx1* in the development of these arteries is probably cell non-autonomous, as the gene is not expressed in structural components of the artery but in the surrounding pharyngeal endoderm. We hypothesized that Tbx1 may trigger signals from the pharyngeal endoderm directed to the underlying mesenchyme. We show that the expression patterns of *Fgf8* and *Fgf10*, which partially overlap with *Tbx1* expression pattern, are altered in *Tbx1*−/− mutants. In particular, *Fgf8* expression is abolished in the pharyngeal endoderm. To understand the significance of this finding for the pathogenesis of the mutant *Tbx1* phenotype, we crossed *Tbx1* and *Fgf8* mutants. Double heterozygous *Tbx1*+/−;*Fgf8*+/− mutants present with a significantly higher penetrance of aortic arch artery defects than do

Tbx1+/−;*Fgf8*+/+ mutants, while *Tbx1*+/+;*Fgf8*+/− animals are normal. We found that *Fgf8* mutation increases the severity of the primary defect caused by *Tbx1* haploinsufficiency, i.e. early hypoplasia of the fourth pharyngeal arch arteries, consistent with the time and location of the shared expression domain of the two genes. Hence, *Tbx1* and *Fgf8* interact genetically in the development of the aortic arch. Our data provide the first evidence of a genetic link between *Tbx1* and FGF signaling, and the first example of a modifier of the *Tbx1* haploinsufficiency phenotype. We speculate that the *FGF8* locus might affect the penetrance of cardiovascular defects in individuals with chromosome 22q11 deletions involving *TBX1*.

Key words: Pharyngeal endoderm, Pharyngeal arch arteries, Phenotypic modifiers

INTRODUCTION

Tbx1, a T-box putative transcription factor, is required for the segmentation of the pharyngeal apparatus, and homozygous mutation causes multiple developmental defects, including cardiovascular, craniofacial, ear, thymic and parathyroid defects (Jerome and Papaioannou, 2001; Lindsay et al., 2001; Vitelli et al., 2002). *Tbx1* expression has been extensively analyzed by RNA in situ hybridization (Chapman et al., 1996; Garg et al., 2001; Jerome and Papaioannou, 2001; Lindsay et al., 2001; Merscher et al., 2001) and by a *lacZ* reporter knocked into the endogenous locus (Vitelli et al., 2002). The expression pattern is dynamic during development and is mainly localized in the head mesenchyme, pharyngeal endoderm, core mesenchyme of the cranial pharyngeal arches, outflow tract of the heart, mesenchyme surrounding the dorsal aortae, otocyst and sclerotome. *Tbx1* haploinsufficiency causes aortic arch patterning defects in mice (Jerome and Papaioannou, 2001; Lindsay et al., 2001; Merscher et al., 2001) of the same type as those observed in a mouse model, named *Df1*/+ of the chromosomal deletion occurring in individuals with DiGeorge

syndrome (Lindsay et al., 1999). The mouse deletion *Df1* and the human deletion *del22q11* both include *Tbx1*, making this gene the most likely candidate for a pathogenetic role in this syndrome.

Tbx1 haploinsufficiency causes early growth and remodeling defects of the fourth pharyngeal arch arteries (PAAs), first evident at embryonic day (E) 10.5. The caudal PAAs (third, fourth and sixth) form sequentially as symmetric vessels connecting the aortic sac with the dorsal aortae. From ~E11.5, the PAAs undergo a major, asymmetric remodeling that leads to the mature aortic arch and great vessel patterning (Srivastava and Olson, 2000). In particular, the left fourth PAA contributes to the section of the mature aortic arch between the origins of the left common carotid artery and the left subclavian artery. Developmental failure of the left fourth PAA causes interruption of the aortic arch type B (IAA-B). The right fourth PAA provides the connection of the right subclavian artery with the innominate artery. Developmental failure of the right fourth PAA causes aberrant origin of the right subclavian artery, most commonly from the descending aorta, via a retroesophageal vessel.

*lac*Z-knock-in experiments have shown that *Tbx1* is not expressed in the structural components of the fourth PAA but in the surrounding pharyngeal endoderm, suggesting that the role of *Tbx1* in the growth of this artery is cell non-autonomous (Vitelli et al., 2002). The fibroblast growth factor (FGF) signaling has been shown to interact with the function of other T-box genes, and the presence of regulatory loops between T-box transcription factors and Fgf genes has been suggested (Casey et al., 1998; Ohuchi et al., 1998; Rodriguez-Esteban et al., 1999; Takeuchi et al., 1999). Therefore, we tested whether FGF signaling could mediate Tbx1 functions especially as it relates to the pathogenesis of cardiovascular defects, the major cause of morbidity and mortality in individuals with DiGeorge syndrome. Our results identify *Fgf8* as the first known genetic interactor of *Tbx1* and suggest that other *Fgf* family members may mediate the role of *Tbx1* in the development of other derivatives of the pharyngeal apparatus.

MATERIALS AND METHODS

Mouse mutants and breeding

The generation of *Tbx1* mice carrying the allele *Tbx1^{tm1Bld}* (referred to as *Tbx1^−*) has already been described (Lindsay et al., 2001). Mutants were maintained on a C57BL/6×129SvEvBrd(129S5) mixed genetic background. *Fgf8^{+/−}* animals (carrying the null allele *Fgf8^{Δ2,3}* (Meyers et al., 1998) originally maintained in a ICR outbred background, were back-crossed twice in a C57BL/6× 129SvEvBrd(129S5) and bred with *Tbx1^{+/−}* mutants. Embryos were collected at embryonic day (E) 18.5 or E10.5, considering E0.5 as the day on which the vaginal plug was observed. Mice or embryos were genotyped by PCR of DNA extracted from tail biopsies or yolk sacs, using previously published PCR primer pairs (Lindsay et al., 2001; Meyers et al., 1998). Phenotype scoring was performed before genotypic analysis.

In situ hybridization

Radioactive or non-radioactive in situ hybridization experiments were performed on sectioned or whole-mount embryos, respectively, using a published protocol (Albrecht et al., 1997). Sense and antisense riboprobes were prepared by reverse transcription of DNA probes and labeled by incorporation of digoxigenin-conjugated UTP (Roche) or ^{35}S-UTP (ICN).

β-Galactosidase detection

Embryos were fixed in paraformaldehyde and then processed for X-gal staining, according to standard procedures. Embryos were photographed as wholemounts and then embedded in paraffin wax and cut in 10 μm histological sections. Sections were counterstained with Nuclear Fast Red.

Ink injection

India ink was injected intracardially in E10.5 embryos using pulled glass needles. To avoid scoring growth delayed embryos, we only considered embryos in which the sixth PAAs could be clearly visualized by ink injection. A total of 8 litters was analyzed, in which 45 embryos were scorable. Three fourth PAA phenotypes were scored: normal (similar or larger size than the third PAA), small (considerably smaller than the third PAA) and non-patent to ink, according to previously published criteria (Lindsay and Baldini, 2001). Embryos showing fourth PAA non-patent to ink were embedded in paraffin wax for histological examination.

Cell death analysis

Cell death was detected on whole mount embryos using Lysotracker (Molecular Probes) essentially as described (Zucker et al., 1999). Embryos were then embedded in paraffin and 10 μm histological sections were examined under a fluorescence microscope.

RESULTS

Fgf8 and *Fgf10* have *Tbx1*-dependent expression domains

The *Tbx1* haploinsufficiency phenotype is characterized by hypoplasia of the fourth PAAs. The abnormalities become apparent from ~E10, soon after the formation of the arteries (Lindsay et al., 2001). *Tbx1* is mainly expressed in the pharyngeal endoderm surrounding the arteries but not in their structural components, suggesting a cell non-autonomous role in the early growth and remodeling of the vessels (Vitelli et al., 2002). We hypothesized that *Tbx1* triggers a molecular signal in the pharyngeal endoderm directed to the underlying mesenchyme to support vessel growth. FGF signaling has been shown to interact with other T-box genes and therefore it is possible that FGF molecules may mediate the role of *Tbx1* in fourth PAA growth. The *Fgf8* gene expression pattern overlaps with that of *Tbx1* in the pharyngeal endoderm around the time when the fourth PAA hypoplasia becomes apparent (Fig. 1A,B). To determine whether the expression of *Fgf8* may be altered in the endoderm of *Tbx1* mutants, we performed in situ hybridization of *Tbx1^{+/−}* embryos at E10 (Fig. 1E-F) and E11.5 (not shown), but no alteration could be detected. However, in situ hybridization is not quantitative and subtle variations in gene expression may not be apparent. Therefore, we tested *Fgf8* expression in *Tbx1^{−/−}* embryos. Results show that in these embryos, the *Fgf8* expression in the pharyngeal endoderm is lost, while the other expression domains are maintained (Fig. 1C,D,G,H). Loss of *Fgf8* in the pharyngeal endoderm may be due to gene downregulation or lack of development/survival of endodermal cells expressing *Fgf8*. Indeed, *Tbx1^{−/−}* mutants have severely hypoplastic pharynx and lack pharyngeal pouches (Jerome and Papaioannou, 2001; Lindsay et al., 2001; Vitelli et al., 2002). To test whether the residual pharyngeal endoderm expresses endodermal markers, we hybridized in situ *Shh*, *Nkx2-5* and *Pax9* on tissue sections. All these markers are robustly expressed in the endoderm of homozygous mutants (not shown). In addition, using our *Tbx1-lacZ*-knock-in allele, we could demonstrate β-gal activity in the endoderm of *Tbx1^{−/−}* embryos, indicating that *Tbx1* function is not required for the contribution of *Tbx1*-expressing cells to the endoderm (Vitelli et al., 2002). Overall, these results suggest that the endoderm of *Tbx1^{−/−}* embryos is properly specified.

In addition to pharyngeal endoderm, *Tbx1* is expressed in the core mesenchyme of pharyngeal arches 1, 2 and 3 (Fig. 2A,C), which are considered to be of paraxial mesoderm derivation. Interestingly, *Fgf10* is also expressed in the core mesenchyme of the arches with a similar pattern (Fig. 2B,D), raising the question of whether *Tbx1* may be required for *Fgf10* expression in this tissue. Indeed, *Fgf10* expression is abolished in the core mesenchyme of arches 1 and 2 of *Tbx1^{−/−}* mutants and, in the first arch, it has a low-level, diffuse expression in the arch mesenchyme (Fig. 2E,F). Pharyngeal arch 3 does not form in these mutants, while pharyngeal arch 2 is hypoplastic and arch 1 is of apparently normal size but is slightly mis-shapen. However, arches 1 and 2 express normal levels (though

with size reduction in the second arch) of mesenchymal markers such as *Dlx2* (Vitelli et al., 2002), *Foxd1* and *Bmp4* (E. A. L. and A. B., unpublished). Core mesenchyme cells that normally express *Tbx1* are also present and normally localized in the arches of *Tbx1*$^{-/-}$ embryos, as shown by β-Gal staining (Vitelli et al., 2002). These results are consistent with at least two interpretations: one is that *Fgf10* expression is downregulated in the core mesenchyme, the other is that *Fgf10*-expressing cells are misplaced and diffused in the arch mesenchyme. *Fgf10* expression is normal in other tissues of *Tbx1*$^{-/-}$ embryos, with one notable exception. *Fgf10* is expressed in a region of splanchnic mesoderm located dorsocaudally to the junction of the outflow tract with the pharyngeal apparatus, in the dorsal wall of the pericardial cavity, *Tbx1*-expressing cells are also present in this region (Fig. 3A-C). *Fgf10*-expressing cells from this region are thought to migrate and contribute to the muscle wall of the outflow tract, as they are part of the anterior or secondary heart field (Kelly et al., 2001; Mjaatvedt et al., 2001; Waldo et al., 2001). This *Fgf10* expression domain could not be detected in *Tbx1*$^{-/-}$ embryos (Fig. 3D), while expression of *Nkx2-5*, also present in the secondary heart field (Waldo et al., 2001), was reduced but conserved (not shown). These results suggest that the *Tbx1* function in outflow tract development, revealed by severe outflow tract defects in *Tbx1*$^{-/-}$ mutants, may be mediated by the FGF signaling in the secondary heart field.

Fgf8 and *Tbx1* interact in vivo

The gene expression data shown above suggest that *Fgf8* may interact with *Tbx1* in the pharyngeal endoderm and be a mediator of the cell non-autonomous role of *Tbx1* in fourth pharyngeal arch artery development. If this is the case, dosage reduction of *Fgf8* should enhance the *Tbx1* haploinsufficiency phenotype. To test this hypothesis, we bred *Tbx1*$^{+/-}$ mice with *Fgf8*$^{+/-}$ mice (Meyers et al., 1998) and scored the phenotype of the progeny at E18.5 in order to understand whether combined heterozygosity affects the mature aortic arch anatomy. A total of 137 embryos were analyzed by dissection of the heart and great vessels and all genotypes were recovered according to mendelian ratio. *Tbx1*$^{+/+}$;*Fgf8*$^{+/+}$ embryos (*n*=30) and *Tbx1*$^{+/+}$;*Fgf8*$^{+/-}$ embryos (*n*=30) were normal. Of the 35 *Tbx1*$^{+/-}$;*Fgf8*$^{+/+}$ embryos analyzed, 11 (27%) presented with aortic arch patterning defects of the types previously described in this mutant and with a similar penetrance previously reported for *Df1*/+ animals (Lindsay and Baldini, 2001), which carry a multi-gene

heterozygous deletion that includes *Tbx1*. *Tbx1*$^{+/-}$;*Fgf8*$^{+/-}$ animals presented with high penetrance of arch defects (50%, *n*=36), significantly higher than that found in *Tbx1*$^{+/-}$;*Fgf8*$^{+/+}$ mutants (*P*=0.036). Interestingly, the type of defects observed was not affected by *Fgf8* mutation (Table 1), all defects were attributable to a failure of the fourth PAA development, only one *Tbx1*$^{+/-}$;*Fgf8*$^{+/+}$ and one *Tbx1*$^{+/-}$;*Fgf8*$^{+/-}$ embryo presented with a ventricular septal defect associated with IAA-B. These were the only intracardiac defects observed in any genotype.
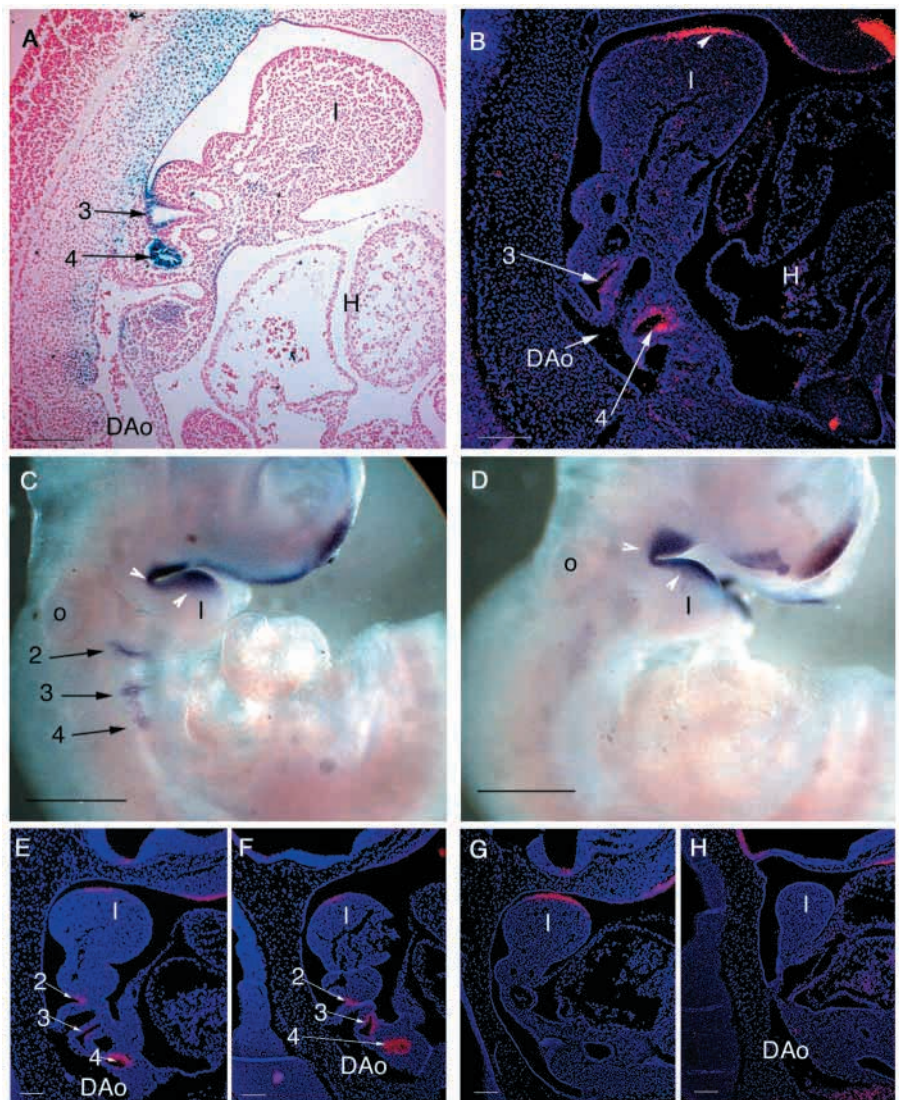
Fig. 1. *Tbx1* and *Fgf8* expression overlaps in the pharyngeal pouches at E10.5. Sagittal sections of an X-gal stained *Tbx1* heterozygous embryo (A) compared with RNA in situ hybridization with *Fgf8* of a wild-type embryo (B) showing a similar expression pattern, particularly in the fourth pharyngeal pouch (4). 3, third pharyngeal pouch; DAo, dorsal aorta; I, first pharyngeal arch; H, heart. Whole-mount in situ hybridization reveals loss of *Fgf8* expression in the pharyngeal endoderm in *Tbx1*$^{-/-}$ (D) when compared with *Tbx1*$^{+/-}$ (C) mutants at E10.5. White arrowheads indicate the expression domain on the ectoderm covering the first arch, which is maintained in both embryos, and is also visible in B. o, otocyst. (E-H) Sagittal sections of an *Fgf8* in situ hybridization of E10 wild-type (E), *Tbx1*$^{+/-}$ (F) and *Tbx1*$^{-/-}$ (G and H, lateral and medial sections, respectively, from the same embryo) embryos. Note the loss of expression in the pharyngeal endoderm of *Tbx1*$^{-/-}$ when compared with E,F, which are essentially identical. For all panels, anterior is upwards and dorsal is leftwards. Scale bars: 100 μm in A-B,E-H; 0.5 mm in C,D.

Table 1. Aortic arch patterning defects in E18.5 embryos

| Genotype	n	Abnormal (%)	IAA-B and RAA	A-RSA	IAA-B, A-RSA and VSD	A-RSA and C-AoA
$Tbx1^{+/+};Fgf8^{+/+}$	30	0	0	0	0	0
$Tbx1^{+/+};Fgf8^{+/-}$	30	0	0	0	0	0
$Tbx1^{+/-};Fgf8^{+/+}$	41	11 (27)	2	6	1	2
$Tbx1^{+/-};Fgf8^{+/-}$	36	18 (50)*	8	6	1	3

*P=0.036.
IAA-B, interrupted aortic arch type B; RAA, right aortic arch; A-RSA, aberrant origin of the right subclavian artery; VSD: Ventricular septal defect. C-AoA: Cervical aortic arch.

The most common abnormality observed in compound heterozygous mutants is an interruption of the aortic arch (type B as it occurs between the left common carotid artery and the left subclavian artery), associated with a retroesophageal connection between the ascending aorta (on the right side of the body axis) and the descending aorta on the left side of the body axis (Fig. 4). Because of this connection, the defect can be described as a right aortic arch (RAA). We interpret the connecting vessel as a compensatory persistence of the embryonic right dorsal aorta, which normally regresses.

To study the early fourth PAA phenotype, we injected ink into the heart of E10.5 embryos obtained from the same breeding scheme indicated above, a total of 56 embryos were scored (Table 2). As previously reported for $Df1$/+ embryos (Lindsay and Baldini, 2001), the penetrance of fourth PAA abnormalities caused by $Tbx1$ haploinsufficiency at E10.5 is much higher than the penetrance of aortic arch defects at E18.5. Out of 14 $Tbx1^{+/-};Fgf8^{+/+}$ embryos

examined, 13 were abnormal; out of 14 $Tbx1^{+/-};Fgf8^{+/-}$ embryos, 13 were abnormal. However, the latter were more severely affected because all but one had bilateral defects, and most had 'absent' fourth PAA phenotype, i.e. were non-patent to ink (Table 2). Indeed, the number of arteries scored as non-patent were significantly higher in $Tbx1^{+/-};Fgf8^{+/-}$ than in $Tbx1^{+/-};Fgf8^{+/+}$ embryos (21 out of 28 and 7 out of 28, respectively, P=0.0002). Histological examination of embryos with fourth PAAs non-patent to ink showed that the arteries were small but present; hence, excluding a defect of formation (not shown). The third and sixth PAAs were normal in all the genotypes. These data indicate that $Tbx1$ and $Fgf8$ interact genetically during the early phases of fourth PAA development, consistent with the time of $Fgf8$ and $Tbx1$ expression overlap in the pharyngeal endoderm. We also examined the progeny of crosses between $Tbx1^{+/-};Fgf8^{+/-}$ and $Tbx1^{+/-};Fgf8^{+/+}$ animals. The cardiovascular phenotype of $Tbx1^{-/-};Fgf8^{+/+}$ and $Tbx1^{-/-};Fgf8^{+/-}$ embryos was essentially identical (n=7 and 5, respectively) (Table 3). Although the number of embryos

Fig. 2. Both $Tbx1$ and $Fgf10$ are expressed in the paraxial mesodermal core of the cranial pharyngeal arches (A-D). Sagittal sections of an X-gal stained $Tbx1$ heterozygous mutant at E10.5 (A,C) compared with RNA in situ hybridization with $Fgf10$ on a wild-type embryo at E10.25 (B,D). In A and B, the $Tbx1$-positive and $Fgf10$-positive paraxial mesoderm (arrows) is seen as a stream of cells entering the first arch mesenchyme (I); o, otocyst. The more medial sections in C,D show the overlap of $Tbx1$ and $Fgf10$ expression in the mesodermal core of the second arch (II) as well (arrows). The arrowhead in D indicates $Fgf10$-positive cells in the ectoderm overlaying the first arch. $Fgf10$ expression in the paraxial mesoderm is absent in $Tbx1$ homozygous mutants at E10.25 (E, left side; F, right side of the same embryo), but is maintained in the first arch ectoderm (arrowhead in E). Some diffuse $Fgf10$ expression is detected in the mesenchyme of the first arch, but not in the hypoplastic second arch ("II"). For all panels, anterior is upwards and dorsal is leftwards. Scale bars: 100 µm.
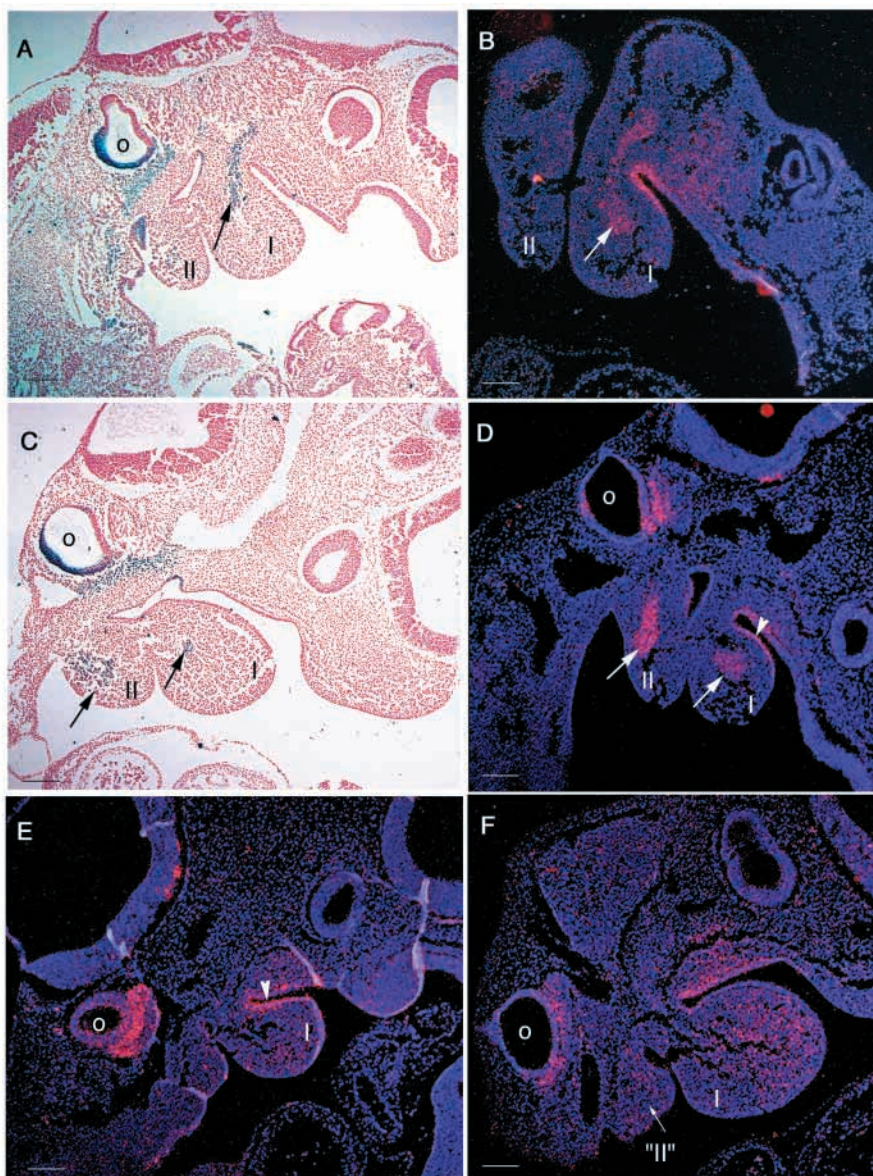
Table 2. Fourth pharyngeal arch artery defects in E10.5 embryos scored by ink injection

| | | | Monolateral | Bilateral | Bilateral defects | | |
| | | | | | Sm/Sm | Sm/N-P | N-P/N-P |
Genotype	*n*	Abn	defect	defect			
Tbx1$^{+/+}$;*Fgf8*$^{+/+}$	18	0	0	0	0	0	0
Tbx1$^{+/+}$;*Fgf8*$^{+/-}$	10	0	0	0	0	0	0
Tbx1$^{+/-}$;*Fgf8*$^{+/+}$	14	13	5	8	1	5	0
Tbx1$^{+/-}$;*Fgf8*$^{+/-}$	14	13	1	12	0	3	9

n, number of scorable embryos (see Materials and Methods); Sm/Sm, both fourth PAAs are thin but patent to ink; Sm/N-P, one artery is thin, the other is not patent to ink; N-P/N-P, both arteries are not patent to ink.

analyzed is small, these results are predicted by the hypothesis that the phenotypically significant interaction between the two genes occurs during the development of the fourth PAAs. Because the fourth PAAs do not form in *Tbx1*$^{-/-}$ animals, the phenotypic enhancing effect of *Fgf8* mutation is pre-empted.

In addition to aortic arch defects, we noticed that at E18.5, 14 out of 30 double heterozygous animals presented with thymic hypoplasia and/or lobe asymmetry (not shown). This phenotype was also seen in six out of 37 *Tbx1*$^{+/-}$;*Fgf8*$^{+/+}$ animals, in three out of 28 *Tbx1*$^{+/+}$;*Fgf8*$^{+/-}$ animals, and in one out of 21 *Tbx1*$^{+/+}$;*Fgf8*$^{+/+}$ animals. Although this phenotype may be in the range of normal variability of the thymus in this genetic background, its penetrance in double heterozygous

mutants is significantly higher than that in the other genotypes (*P*=0.0068). Because *Fgf8*$^{neo/-}$ embryos (where *Fgf8*^{neo} is a hypomorphic allele) also present with thymic defects, including hypoplasia (Abu-Issa et al., 2002), and because the thymus primordia develop from the third pharyngeal pouch where both *Tbx1* and *Fgf8* are expressed (Fig. 1A,B), it is likely that the thymic phenotype in double heterozygous mutants is also a sign of *Tbx1*-*Fgf8* interaction in the pharyngeal endoderm.

Complete loss of function of *Tbx1* causes migration defects of neural crest cells (Vitelli et al., 2002), while severe reduction of Fgf8 dose in *Fgf8*$^{neo/-}$ animals causes increased neural crest cell death (Abu-Issa et al., 2002). To test whether compound
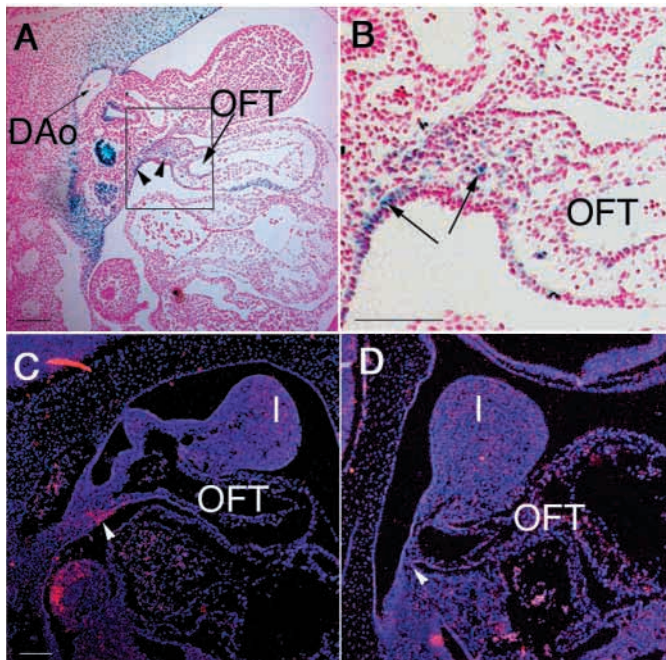
Fig. 3. *Tbx1* and *Fgf10* expression is similar in the presumptive secondary heart field. (A) An X-gal stained *Tbx1*$^{+/-}$ embryo at E10.5 showing positive cells in the dorsal wall of the pericardiac cavity, adjacent to and extending into the outflow tract (OFT; arrowheads in A, arows in B). DAo, dorsal aorta. B is an enlargement of the boxed area in A. (C) RNA in situ hybridization of *Fgf10* on a wild-type E10.5 embryo; arrowhead indicates a cluster of cells thought to contribute to the OFT muscle wall. This cell population is missing in a stage-matched *Tbx1* homozygous mutant (arrowhead in D indicates a comparable region of mesenchyme); I, first pharyngeal arch. Anterior is upwards and dorsal is leftwards in all panels. Scale bars: 100 μm.
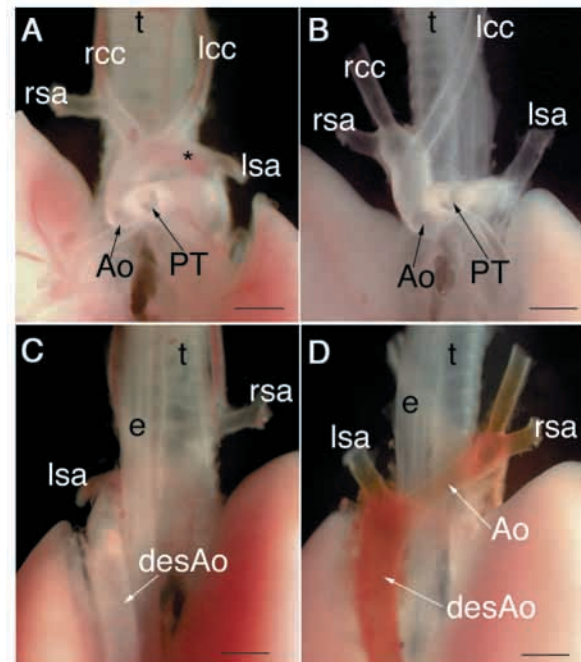
Fig. 4. Normal great vessel anatomy (A,C) compared with the most common defect observed in *Tbx1*$^{+/-}$;*Fgf8*$^{+/-}$ animals (B,D) at E18.5 in dissected heart-lung preparations; anterior is upwards. The frontal view (A,B) reveals lack of a segment of the arch (indicated by an asterisk in A), a type B interruption. The dorsal view (C,D) shows a retro-esophageal connection between the ascending and descending aorta (desAo), probably cause by abnormal persistence of the right dorsal aorta; diluted iodine solution was injected into the aorta in D as a visual aid. Ao, aorta; PT, pulmonary trunk; rcc and lcc, right and left common carotid arteries; rsa and lsa, right and left subclavian arteries; t, trachea; e, esophagus. Scale bars: 1 mm.

Table 3. Cardiovascular phenotype in Tbx1⁻/⁻ E18.5 embryos

Genotype	n	Abnormal	TAC and RAA	TAC and LAA	VSD	AbSCA	AbPA	Other
Tbx1⁻/⁻;Fgf8⁺/⁺	7	7	3	4	7	7	1	2*
Tbx1⁻/⁻;Fgf8⁺/⁻	5	5	3	2	5	5	2	0

TAC, truncus arteriosus communis; RAA, right aortic arch; LAA, left aortic arch; VSD, ventricular septal defect; AbSCA, aberrant origin of subclavian arteries; AbPAs, aberrant origin of pulmonary arteries; *, one case with mitral stenosis and one case with atrioventricular canal.

heterozygosity may be associated with neural crest migration defects, or increased apoptosis of neural crest cells, we have examined double heterozygous E9.5-E10.5 embryos and compared them with wild type and single mutants. Neural crest migration was tested by in situ hybridization with *Crabp1* and cell death by staining with Lysotracker. These tests produced very similar results in all the genotypes tested, suggesting that either potential differences are below the sensitivity of the methods used, or that the *Fgf8* modifier effect is independent from neural crest cell migration or survival.

DISCUSSION

The haploinsufficiency phenotype of the multigene deletion mutant *Df1/+* recapitulates several aspects of the DiGeorge/*del22q11* syndrome, including cardiovascular defects (Lindsay et al., 1999), thymic and parathyroid abnormalities (Taddei et al., 2001), and behavioral abnormalities (Paylor et al., 2001). The haploinsufficient gene responsible for the cardiovascular defects of *Df1/+* mice is *Tbx1* (Jerome and Papaioannou, 2001; Lindsay et al., 2001; Merscher et al., 2001), while the genes responsible for the other aspects of the *Df1*-associated phenotype are still to be identified. An important aspect of the human syndrome is phenotypic variability, which contrasts with a remarkable homogeneity of the genetic defect (Lindsay, 2001; McDermid and Morrow, 2002). The heterogeneity of the clinical picture is due mainly to reduced penetrance of individual clinical findings and, to a lesser extent, to variable expressivity (Matsuoka et al., 1998). We have shown that the reduced penetrance of aortic arch defects in *Df1/+* mice is related to 'recovery' from hypoplasia of the fourth PAA, mostly occurring between E10.5 and E11.5 (Lindsay and Baldini, 2001). At E10.5, all the mutant embryos have at least one of the two fourth PAAs affected. The same phenomenon occurs in *Tbx1⁺/⁻* animals (I. T. and E. A. L., unpublished). This recovery process is, at least in part, under genetic control, as it is affected by the genetic background of animals (Taddei et al., 2001). Our data indicate that *Fgf8* mutation enhances the primary defect of *Tbx1⁺/⁻*, i.e. fourth PAA hypoplasia. Hence, this is a different mechanism from that underlying penetrance differences caused by genetic background.

Severe reduction of *Fgf8* activity in *Fgf8*ⁿᵉᵒ/⁻ embryos causes abnormalities of the third, fourth and sixth PAAs, thymic defects, as well as other abnormalities (Abu-Issa et al., 2002). By contrast, the phenotypic enhancing effects of *Fgf8* heterozygous mutation on *Tbx1* haploinsufficiency is restricted to the fourth PAA and to the thymus, consistent with expression overlap of the two genes in the fourth and third pouches. A phenotypic effect on the third and sixth PAA, which are also

close to the third and fourth pouches, may require further reduction of Fgf8 and/or Tbx1 proteins.

The nature of *Tbx1-Fgf8* interactions remains to be clarified, the *Fgf8* promoter/enhancer elements have not been fully characterized, nor has the exact DNA binding site and transcription activity of the *Tbx1* protein. A direct induction of *Fgf8* by *Tbx1* is possible, but it would be restricted to the pharyngeal endoderm because the expression of the two genes does not overlap in any other tissue. While this hypothesis is simple and consistent with phenotypic observations, it is also possible that the *Tbx1-Fgf8* interaction is non-specific. For example, Fgf8 dose reduction may have a generic negative impact on arch mesenchymal cells, for example, aggravating the development of an already compromised fourth PAA. We think that this scenario is unlikely because (1) *Tbx1* is required for the expression of at least two *Fgf* genes in shared expression domains, suggesting specific interactions with FGF signaling, and (2) *Fgf8*ⁿᵉᵒ/⁻ embryos have fourth PAA defects (Abu-Issa et al., 2002), indicating that Fgf8 contributes to the development of these arteries.

We propose that FGF signaling mediates the role of *Tbx1* in the development of various derivatives of the pharyngeal arches and pouches, and perhaps different Fgf genes may be involved in the development of different derivatives. We have shown here that *Fgf8* interacts with *Tbx1* in aortic arch and in thymic development in vivo. *Tbx1⁻/⁻* mice do not have thymus (Jerome and Papaioannou, 2001; Lindsay et al., 2001) and *Df1/+* mice, in certain genetic backgrounds, have thymic hypoplasia (Taddei et al., 2001). We have also shown that *Fgf10* expression is affected in *Tbx1⁻/⁻* mice in the core mesenchyme and in the secondary heart field. *Fgf10* is required for lung, limb (Min et al., 1998; Sekine et al., 1999) and thymic development (Revest et al., 2001), but the cardiovascular phenotype in *Fgf10⁻/⁻* has not been described. It would be of interest to cross-breed *Tbx1* and *Fgf10* mutants, when available, to investigate whether the two genes interact during outflow tract and/or thymic development.

The significance of our findings for DiGeorge/*del22q11* syndrome remains to be addressed. Our data should prompt the analysis of FGF loci to establish whether allelic variants are associated with increased risk of cardiovascular defects, thymic defects, or other pharyngeal pouch/arch developmental abnormalities in individuals with *del22q11* syndrome.

REFERENCES

Abu-Issa, R., Smyth, G., Smoak, I., Yamamura, K.-I. and Meyers, E. N. (2002). Fgf8 is required for pharyngeal arch development and cardiovascular patterning in the mouse. *Development* **129**, 4613-4625.

Albrecht, U., Eichele, G., Helms, J. A. and Lu, H. C. (1997). Visualization of gene expression patterns by in situ hybridization. In *Molecular and Cellular Methods in Developmental Toxicology* (ed. G. P. Daston), pp. 23-48. New York: CRC Press.

Casey, E. S., O'Reilly, M. A., Conlon, F. L. and Smith, J. C. (1998). The T-box transcription factor Brachyury regulates expression of eFGF through binding to a non-palindromic response element. *Development* **125**, 3887-3894.

Chapman, D. L., Garvey, N., Hancock, S., Alexiou, M., Agulnik, S. I., Gibson-Brown, J. J., Cebra-Thomas, J., Bollag, R. J., Silver, L. M. and Papaioannou, V. E. (1996). Expression of the T-box family genes, Tbx1-Tbx5, during early mouse development. *Dev. Dyn.* **206**, 379-390.

Garg, V., Yamagishi, C., Hu, T., Kathiriya, I. S., Yamagishi, H. and Srivastava, D. (2001). Tbx1, a DiGeorge syndrome candidate gene, is regulated by sonic hedgehog during pharyngeal arch development. *Dev. Biol.* **235**, 62-73.

Jerome, L. A. and Papaioannou, V. E. (2001). DiGeorge syndrome phenotype in mice mutant for the T-box gene, *Tbx1*. *Nat. Genet.* **27**, 286-291.

Kelly, R. G., Brown, N. A. and Buckingham, M. E. (2001). The arterial pole of the mouse heart forms from Fgf10-expressing cells in pharyngeal mesoderm. *Dev. Cell* **1**, 435-440.

Lindsay, E. A. (2001). Chromosomal microdeletions: Dissecting del22q11 syndrome. *Nat. Rev. Genet.* **2**, 858-868.

Lindsay, E. A. and Baldini, A. (2001). Recovery from arterial growth delay reduces penetrance of cardiovascular defects in mice deleted for the DiGeorge syndrome region. *Hum. Mol. Genet.* **10**, 997-1002.

Lindsay, E. A., Botta, A., Jurecic, V., Carattini-Rivera, S., Cheah, Y.-C., Rosenblatt, H. M., Bradley, A. and Baldini, A. (1999). Congenital heart disease in mice deficient for the DiGeorge syndrome region. *Nature* **401**, 379-383.

Lindsay, E. A., Vitelli, F., Su, H., Morishima, M., Huynh, T., Pramparo, T., Jurecic, V., Ogunrinu, G., Sutherland, H. F., Scambler, P. J. et al. (2001). Tbx1 haploinsufficieny in the DiGeorge syndrome region causes aortic arch defects in mice. *Nature* **410**, 97-101.

Matsuoka, R., Kimura, M., Scambler, P. J., Morrow, B. E., Imamura, S., Minoshima, S., Shimizu, N., Yamagishi, H., Joh-o, K., Watanabe, S. et al. (1998). Molecular and clinical study of 183 patients with conotruncal anomaly face syndrome. *Hum. Genet.* **103**, 70-80.

McDermid, H. E. and Morrow, B. E. (2002). Genomic disorders on 22q11. *Am. J. Hum. Genet.* **70**, 1077-1088.

Merscher, S., Funke, B., Epstein, J. A., Heyer, J., Puech, A., Min Lu, M. M., Xavier, R. J., Demay, M. B., Russell, R. G., Factor, S. et al. (2001). TBX1 Is Responsible for Cardiovascular Defects in Velo-Cardio-Facial/DiGeorge Syndrome. *Cell* **104**, 619-629.

Meyers, E. N., Lewandoski, M. and Martin, G. R. (1998). An Fgf8 mutant allelic series generated by Cre- and Flp-mediated recombination. *Nat. Genet.* **18**, 136-141.

Min, H., Danilenko, D. M., Scully, S. A., Bolon, B., Ring, B. D., Tarpley, J. E., DeRose, M. and Simonet, W. S. (1998). Fgf-10 is required for both limb and lung development and exhibits striking functional similarity to Drosophila branchless. *Genes Dev.* **12**, 3156-3161.

Mjaatvedt, C. H., Nakaoka, T., Moreno-Rodriguez, R., Norris, R. A., Kern, M. J., Eisenberg, C. A., Turner, D. and Markwald, R. R. (2001). The outflow tract of the heart is recruited from a novel heart-forming field. *Dev. Biol.* **238**, 97-109.

Ohuchi, H., Takeuchi, J., Yoshioka, H., Ishimaru, Y., Ogura, K., Takahashi, N., Ogura, T. and Noji, S. (1998). Correlation of wing-leg identity in ectopic FGF-induced chimeric limbs with the differential expression of chick Tbx5 and Tbx4. *Development* **125**, 51-60.

Paylor, R., McIlwain, K. L., McAninch, R., Nellis, A., Yuva-Paylor, L. A., Baldini, A. and Lindsay, E. A. (2001). Mice deleted for the DiGeorge/velocardiofacial syndrome region show abnormal sensorimotor gating and learning and memory impairments. *Hum. Mol. Genet.* **10**, 2645-2650.

Revest, J. M., Suniara, R. K., Kerr, K., Owen, J. J. and Dickson, C. (2001). Development of the thymus requires signaling through the fibroblast growth factor receptor R2-IIIb. *J. Immunol.* **167**, 1954-1961.

Rodriguez-Esteban, C., Tsukui, T., Yonei, S., Magallon, J., Tamura, K. and Izpisua Belmonte, J. C. (1999). The T-box genes Tbx4 and Tbx5 regulate limb outgrowth and identity. *Nature* **398**, 814-818.

Sekine, K., Ohuchi, H., Fujiwara, M., Yamasaki, M., Yoshizawa, T., Sato, T., Yagishita, N., Matsui, D., Koga, Y., Itoh, N. et al. (1999). Fgf10 is essential for limb and lung formation. *Nat. Genet.* **21**, 138-141.

Srivastava, D. and Olson, E. N. (2000). A genetic blueprint for cardiac development. *Nature* **407**, 221-226.

Taddei, I., Morishima, M., Huynh, T. and Lindsay, E. A. (2001). Genetic factors are major determinants of phenotypic variability in a mouse model of the DiGeorge/del22q11 syndromes. *Proc. Natl. Acad. Sci. USA* **98**, 11428-11431.

Takeuchi, J. K., Koshiba-Takeuchi, K., Matsumoto, K., Vogel-Hopker, A., Naitoh-Matsuo, M., Ogura, K., Takahashi, N., Yasuda, K. and Ogura, T. (1999). Tbx5 and Tbx4 genes determine the wing/leg identity of limb buds. *Nature* **398**, 810-814.

Vitelli, F., Morishima, M., Taddei, I., Lindsay, E. A. and Baldini, A. (2002). Tbx1 mutation causes multiple cardiovascular defects and disrupts neural crest and cranial nerve migratory pathways. *Hum. Mol. Genet.* **11**, 915-922.

Waldo, K. L., Kumiski, D. H., Wallis, K. T., Stadt, H. A., Hutson, M. R., Platt, D. H. and Kirby, M. L. (2001). Conotruncal myocardium arises from a secondary heart field. *Development* **128**, 3179-3188.

Zucker, R. M., Hunter, E. S., 3rd and Rogers, J. M. (1999). Apoptosis and morphology in mouse embryos by confocal laser scanning microscopy. *Methods* **18**, 473-480.